



OPEN

In vitro kinase assay reveals ADP-heptose-dependent ALPK1 autophosphorylation and altered kinase activity of disease-associated ALPK1 mutants

Diego García-Weber^{1,3}, Anne-Sophie Dangeard^{1,3}, Veronica Teixeira¹, Martina Hauke², Alexis Carreaux¹, Christine Josenhans² & Cécile Arrieumerlou¹✉

Alpha-protein kinase 1 (ALPK1) is a pathogen recognition receptor that detects ADP-heptose (ADPH), a lipopolysaccharide biosynthesis intermediate, recently described as a pathogen-associated molecular pattern in Gram-negative bacteria. ADPH binding to ALPK1 activates its kinase domain and triggers TIFA phosphorylation on threonine 9. This leads to the assembly of large TIFA oligomers called TIFAsomes, activation of NF- κ B and pro-inflammatory gene expression. Furthermore, mutations in *ALPK1* are associated with inflammatory syndromes and cancers. While this kinase is of increasing medical interest, its activity in infectious or non-infectious diseases remains poorly characterized. Here, we use a non-radioactive ALPK1 in vitro kinase assay based on the use of ATP γ S and protein thiophosphorylation. We confirm that ALPK1 phosphorylates TIFA T9 and show that T2, T12 and T19 are also weakly phosphorylated by ALPK1. Interestingly, we find that ALPK1 itself is phosphorylated in response to ADPH recognition during *Shigella flexneri* and *Helicobacter pylori* infection and that disease-associated ALPK1 mutants exhibit altered kinase activity. In particular, T237M and V1092A mutations associated with ROSAH syndrome and spiradenoma/spiradenocarcinoma respectively, exhibit enhanced ADPH-induced kinase activity and constitutive assembly of TIFAsomes. Altogether, this study provides new insights into the ADPH sensing pathway and disease-associated ALPK1 mutants.

Alpha-protein kinase 1 (ALPK1, or lymphocyte alpha-kinase, LAK) is a kinase that is attracting growing interest because it recently appeared to be involved in important biological processes in health and disease. It belongs to the human alpha-kinase (α -kinase) family, a subset of six atypical kinases that share little sequence similarity in their catalytic domain with conventional kinases and which instead, have a kinase domain whose architecture is homologous to that of the myosin heavy chain kinases of *Dictyostelium discoideum*¹. ALPK1 is a 139 kDa protein that contains an N-terminal alpha helical domain, an unstructured linker region and a C-terminal α -kinase domain. Like all members of the α -kinase family, it appeared recently in evolution and is only found in eukaryotes. ALPK1 was initially described as a protein involved in epithelial cell polarity and exocytic vesicular transport towards the apical plasma membrane². Indeed, Heine et al. showed that this kinase resides on Golgi-derived vesicles where it phosphorylates myosin IA, an apical vesicle transport motor protein that regulates the delivery of vesicles to the plasma-membrane². ALPK1 has also been shown to phosphorylate myosin IIA and thereby modulate TNF- α trafficking in gout flares³. More recently, our laboratory identified a role of ALPK1 in innate immunity during bacterial infection⁴. Indeed, we showed that this atypical kinase controls the oligomerization of TIFA and TRAF6 proteins, a process that activates the transcription factor NF- κ B and

¹Université Paris Cité, CNRS, INSERM, Institut Cochin, 75014 Paris, France. ²Max von Pettenkofer Institute, Ludwig Maximilians Universität München, Pettenkoferstrasse 9a, 80336 Munich, Germany. ³These authors contributed equally: Diego García-Weber and Anne-Sophie Dangeard. ✉email: cecile.arrieumerlou@inserm.fr

induces the expression of inflammatory genes during infection by the Gram-negative bacteria *Shigella flexneri*, *Salmonella Typhimurium* and *Neisseria meningitidis*⁴. TIFA is a 20-kDa adaptor protein, which was first identified as a TRAF6-binding protein involved in NF- κ B activation⁵. It contains a conserved threonine in position 9 (T9), a forkhead-associated (FHA) domain responsible for the recognition of phosphorylated threonine and serine residues and a glutamic acid at position 178 involved in TRAF6 binding. In resting conditions, TIFA is found as an intrinsic dimer⁶. After phosphorylation by ALPK1⁷, phosphorylated T9 (pT9) residues are recognized by FHA domains of adjacent dimers, leading to the formation of large TIFA oligomers, called TIFAsomes. We and others have shown that ADP-L-glycero- β -D-manno-heptose (ADPH), a soluble metabolite of the Gram-negative lipopolysaccharide (LPS) biosynthetic pathway, is the pathogen-associated molecular pattern (PAMP) whose recognition triggers the activation of the ALPK1/TIFA axis⁷⁻⁹. In addition, Zhou et al. showed that ALPK1 is the PRR for ADPH and characterized the binding site of ADPH on the N-terminal domain (NTD) of ALPK1 by crystal structure analysis⁷. They found that the NTD harbors 18 α -helices with 14 of them assembled into 7 antiparallel pairs that form a right-hand solenoid. ADPH binds in a pocket present on the concave side of the solenoid and several residues of ALPK1 interact with ADPH. Structural data suggest that the binding of ADPH to the NTD of ALPK1 interferes with the interactions that this domain has with residues of the kinase domain, which are predicted to be located near the kinase catalytic cleft⁷. This mechanism may induce a conformational change, which would make the catalytic cleft more exposed, thereby promoting the kinase activity of ALPK1. In addition to *S. flexneri*, *S. Typhimurium* and *N. meningitidis*, the ALPK1/TIFA axis is activated during infection with *Yersinia pseudotuberculosis*⁷, *Helicobacter pylori*¹⁰⁻¹² and *Campylobacter jejuni*¹³, showing that ALPK1 is involved in innate immunity against important human Gram-negative pathogens.

Beyond its role during infection, ALPK1 is also involved in the control of intestinal homeostasis. Indeed, ALPK1 was identified as the main intestinal inflammation regulator of the *Helicobacter hepaticus*-induced colitis and associated cancer susceptibility locus in mice¹⁴.

Finally, several publications reported a link between single-nucleotide polymorphisms or short deletion mutations in the *ALPK1* gene and disease susceptibility. Diseases include recurrent periodic fever¹⁵, ROSAH syndrome¹⁶, chronic kidney disease¹⁷, myocardial infarction¹⁸, ischemic stroke¹⁹, lung and colorectal cancer²⁰, spiradenoma and adenocarcinoma²¹, Type 2 Diabetes Mellitus and gout^{19,22} and interestingly, most of them share an inflammatory component. Whether mutations associated with these diseases alter the kinase activity of ALPK1 is unknown.

Although ALPK1 is involved in important biological processes, measurements of its kinase activity in infectious and non-infectious contexts were only partially addressed. Here, we use a versatile non-radioactive in vitro kinase assay based on the use of ATP γ S and protein thiophosphorylation reactions. We confirm that ALPK1 phosphorylates TIFA at position T9 and address the phosphorylation of additional TIFA residues. Furthermore, we report that ALPK1 itself is phosphorylated after ADPH recognition upon exposure to pathogens and that disease-associated ALPK1 mutants exhibit altered kinase activity.

Results

ADPH induces TIFA T9 phosphorylation, TIFAsome assembly and NF- κ B activation in an ALPK1-dependent manner. In response to ADPH recognition, ALPK1 phosphorylates TIFA proteins on T9 residues⁷. Consecutively, inter-molecular binding of pT9 to FHA domains of TIFA dimers induces the formation of large TIFAsomes, a process that results in the oligomerization of TRAF6 and the activation of NF- κ B. The formation of TIFAsomes can be visualized in HeLa cells expressing GFP-TIFA whereas the activation of NF- κ B is measured by monitoring the nuclear translocation of p65 by immunofluorescence. The role of ALPK1 in ADPH sensing is confirmed in Fig. 1 showing that the formation of TIFAsomes induced by ADPH treatment was inhibited in hALPK1 siRNA-transfected cells compared to control cells (Fig. 1A,B). In line with this result, ADPH-induced NF- κ B p65 nuclear translocation was also altered in ALPK1-depleted cells (Fig. 1A) as quantified by measuring the cytosolic/nuclear p65 fluorescence intensity ratio by automated image analysis (Fig. 1C). As expected, depleting ALPK1 did not affect TNF α -induced p65 nuclear translocation (Fig. 1A,C). In order to directly address the role of ALPK1 in pT9 phosphorylation, HEK293 cells were transfected or not with a wild-type (wt) myc-hALPK1 cDNA construct and ALPK1 was immunoprecipitated using an anti-myc antibody. It was then incubated with purified GST-TIFA in the presence of ATP and analysed by western blot using the previously described anti-pT9 antibody⁷. Data confirmed that ALPK1 induced the phosphorylation of TIFA on T9 residues in response to the recognition of ADPH (Fig. 1D,E and Supplementary Fig. S1). Altogether, these results confirmed that ADPH sensing induces TIFA T9 phosphorylation, TIFAsome assembly and subsequent NF- κ B activation in an ALPK1-dependent manner.

An in vitro kinase assay based on protein thiophosphorylation reveals the phosphorylation of ALPK1 in response to ADPH sensing. The development of an anti-pT9 antibody was decisive in the analysis of the ALPK1/TIFA axis. However, since its usage is limited to the analysis of TIFA phosphorylation on threonine 9 residues, it does not allow the identification of alternative phosphorylation sites on TIFA, nor any other ALPK1 potential substrates. Here, we used an in vitro ALPK1 kinase assay based on the use ATP γ S and the measurement of protein thiophosphorylation reactions. ATP γ S is a non-hydrolysable ATP analogue that can be utilized to transfer a thiophosphate group containing a sulfur atom at position gamma on a substrate. Although the vast majority of kinases can use ATP γ S as a phosphodonor, this often occurs with reduced catalytic rate compared to ATP²³. Briefly, HEK293 cells were transfected with a cDNA construct encoding myc-hALPK1 and, 48 h later, were treated or not with ADPH. ALPK1 was immunoprecipitated with an anti-myc antibody and, to validate the assay, was incubated with its known substrate, purified GST-TIFA, in the presence of ATP γ S at 37 °C for 1 h to allow protein thiophosphorylation. This critical step was followed

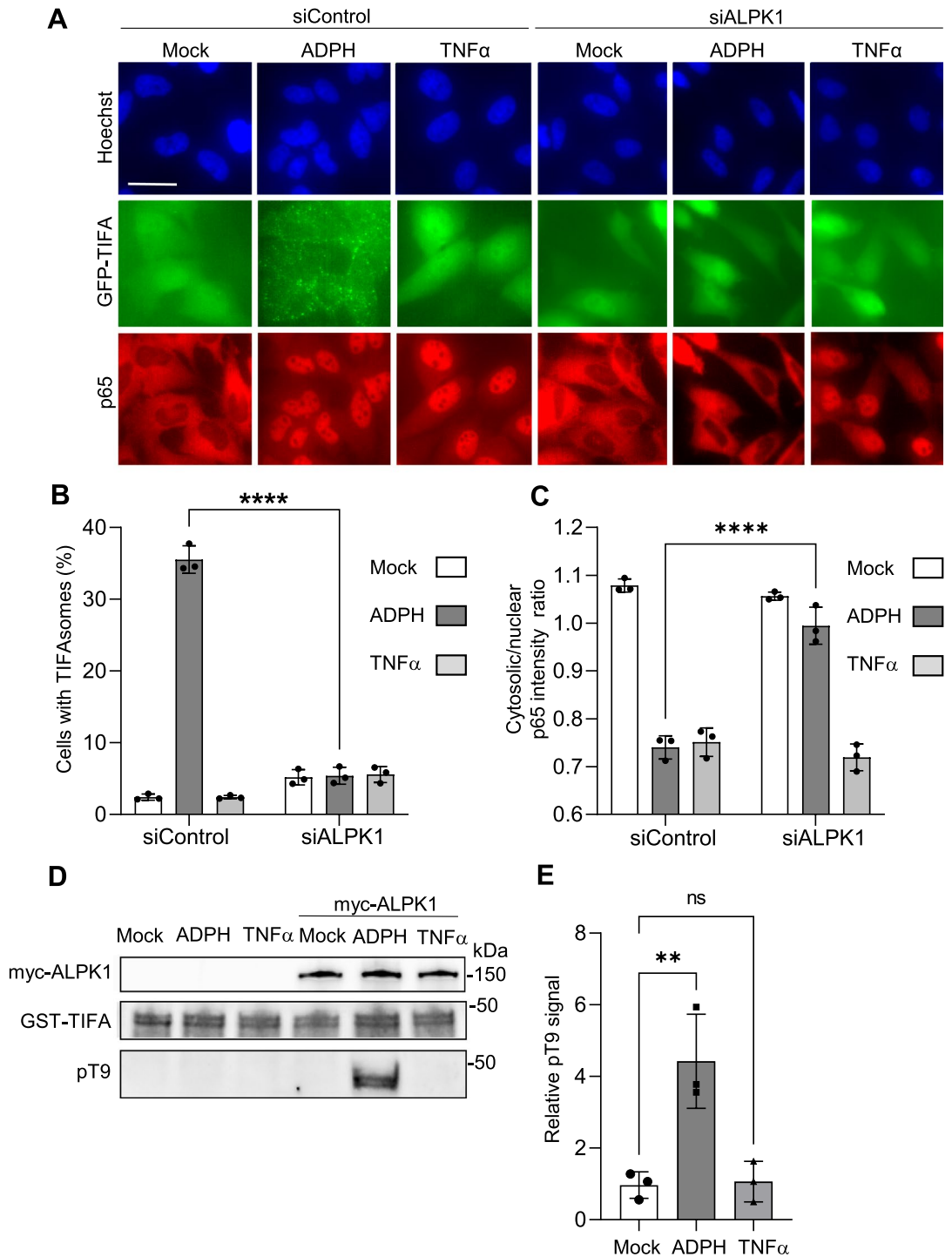


Figure 1. ADPH induces TIFA T9 phosphorylation, TIFAsome assembly and NF- κ B activation in an ALPK1-dependent manner. **(A)** ADPH-induced TIFAsome assembly and NF- κ B nuclear translocation are ALPK1-dependent. HeLa GFP-TIFA expressing cells were transfected with control or ALPK1 siRNAs and treated or not with ADPH or TNF α for 1 h. They were then stained for p65 NF- κ B (in red) and DNA with Hoechst (in blue). GFP-TIFA is shown in green. Bar scale is 10 μ m. **(B)** Quantification of the fraction of cells with TIFAsomes as shown in **(A)**. **(C)** Quantification of p65 NF- κ B nuclear translocation as shown in **(A)**. p65 translocation was quantified by measuring the p65 intensity ratio between the cytoplasm and the nucleus by automated image analysis. **(D)** In response to ADPH sensing, ALPK1 phosphorylates TIFA at position T9. HEK293 cells were transfected or not with a wt myc-hALPK1 cDNA construct and stimulated or not with ADPH or TNF α for 1 h. ALPK1 was immunoprecipitated and used in a GST-TIFA phosphorylation assay. myc-ALPK1, GST-TIFA and pT9 were detected by western blot with anti-myc, anti-GST and anti-pT9 antibodies, respectively. **(E)** Quantification of TIFA T9 phosphorylation as shown in **(D)**. pT9 is quantified by measuring the ratio between pT9 and total GST-TIFA. All data correspond to the mean \pm SD of 3 independent experiments. Statistical significance was assessed using two-way ANOVA **(B,C)** followed by Tukey's multiple comparisons test or one-way ANOVA followed by Dunnett's multiple comparisons test **(E)** ** $P < 0.01$, **** $P < 0.0001$, not significant (ns).

by an alkylation reaction carried out by adding the alkylating reagent p-nitrobenzyl mesylate (PNBM) to the assay. Thus, thioester-type covalent bonds are formed at the locations occupied by the thiophosphate groups of the substrate and these can be detected by an anti-thiophosphate ester antibody (pTE) in western blots as previously described²⁴. As expected, ADPH treatment induced the thiophosphorylation of GST-TIFA and this process was dependent on the presence of ATP γ S and the alkylating reagent PNBM in the assay (Fig. 2A,B and Supplementary Fig. S2). It was also dependent on the presence of myc-ALPK1, strongly indicating that TIFA thiophosphorylation resulted from ALPK1 kinase activity (Fig. 2C,D and Supplementary Fig. S3). Interestingly, a band corresponding to myc-hALPK1 was also detected by the anti-thiophosphate ester antibody, showing that ALPK1 was also thiophosphorylated in response to the recognition of ADPH (Fig. 2A,C). As for TIFA, ALPK1 thiophosphorylation was dependent on ATP γ S and PNBM. Interestingly, the mechanism of ALPK1 thiophosphorylation observed in response to ADPH sensing was independent on the presence of GST-TIFA in the assay (Fig. 2C). In order to further characterize this new finding, we tested whether ALPK1 thiophosphorylation was dependent on the kinase activity of ALPK1. Cells were transfected with cDNA constructs encoding myc-ALPK1 wt, kinase (Δ K) or N-terminal (Δ N) domain deleted mutants, or with a K1067R mutant whose kinase activity is abolished⁷. As expected, ADPH-induced TIFA thiophosphorylation was abolished in cells expressing the different ALPK1 mutants (Fig. 2E,F and Supplementary Fig. S4). Interestingly, ALPK1 thiophosphorylation was also abolished in these cells, showing that ADPH binding and ALPK1 kinase activity were both required for ALPK1 thiophosphorylation. Altogether, our ALPK1 activity assay based on protein thiophosphorylation confirmed that TIFA is a substrate of ALPK1, and revealed the phosphorylation of ALPK1 in response to ADPH sensing. Since the latter process is strictly dependent on the kinase activity of ALPK1, our results strongly suggest that the phosphorylation of ALPK1 results from an autophosphorylation mechanism.

S. flexneri and H. pylori infections induce the phosphorylation of ALPK1. In order to test whether ALPK1 is phosphorylated during bacterial infection, HeLa cells were infected with the enteroinvasive bacterium *S. flexneri* at different multiplicities of infection (MOIs) and the thiophosphorylation status of GST-TIFA and myc-ALPK1 was analysed as described above. Consistent with data obtained in ADPH-treated cells, both proteins were increasingly thiophosphorylated with increasing MOIs (Fig. 3A–C and Supplementary Fig. S5). Interestingly, their thiophosphorylation was sustained for several hours post infection (Fig. 3D,E and Supplementary Fig. S6), indicating that the mechanism of ADPH sensing was likely active for this period in *S. flexneri* infected cells. TIFA and ALPK1 were also thiophosphorylated in epithelial cells infected with wild-type *Helicobacter pylori*, whereas an *hldE* gene deletion mutant (Δ *hldE*), unable to synthesize ADPH⁹, failed to do so (Fig. 3F–H and Supplementary Fig. S7). Altogether, these results showed that the mechanism of ADPH sensing that occurs during bacterial infection induces the phosphorylation of both TIFA and ALPK1.

ALPK1 phosphorylates TIFA on multiple residues. A kinase assay based on protein thiophosphorylation allows to investigate kinase activity on any potential substrates, so we further explored the substrate specificity of ALPK1. First, ALPK1's ability to phosphorylate myelin basic protein (MBP) was monitored. MBP is a substrate commonly used in in vitro kinase assays, including those for MAPK, PKA, PKC cyclin-dependent and calmodulin-dependent protein kinases^{25–27}. In contrast to TIFA, MBP was not thiophosphorylated in response to ADPH-dependent activation of ALPK1 (Fig. 4A,B and Supplementary Fig. S8), suggesting that the kinase activity of ALPK1 is substrate specific. As TIFA is an important substrate of ALPK1, we also thoroughly explored its phosphorylation. In particular, we tested whether T9 is the only residue phosphorylated by ALPK1. To address this point, T9 and several amino acids surrounding T9 were individually mutated to alanine. Corresponding recombinant GST-TIFA proteins were produced in *Escherichia coli*, purified and used as substrates in thiophosphorylation-based ALPK1 kinase assay. As expected, thiophosphorylation was reduced for the T9A mutant, confirming that T9 is phosphorylated by ALPK1 (Fig. 4C–E and Supplementary Fig. S9). Interestingly, it was not completely abolished, indicating that thiophosphorylation also occurred on other TIFA residues. Quantification of normalized pTE GST-TIFA signals showed that thiophosphorylation was very slightly reduced for T2A, T12A and T19A but the effects were not statistically significant compared to wt (Fig. 4E). To further characterize the potential phosphorylation of these residues, a T2A, T12A, T19A and T9A quadruple mutant was generated and used as ALPK1 substrate. When these four residues were mutated to alanine, thiophosphorylation was entirely abolished in a significant manner (Fig. 4F,G and Supplementary Fig. S10), confirming that they were likely phosphorylated by ALPK1. In contrast to T9A, individual T2A, T12A and T19A mutants were all able to assemble into TIFAsomes in response to ADPH recognition during *S. flexneri* infection (Supplementary Fig. S11). Taken together, these results show that, in addition to T9, several surrounding residues can be weakly phosphorylated by ALPK1. However, the phosphorylation of these residues is not necessary for the formation of TIFAsomes in response to ADPH sensing.

Several disease-associated ALPK1 mutants have altered kinase activity. Mutations in ALPK1 have been recently described as associated or responsible for diseases, including inflammatory disorders and cancers. Therefore, we used the thiophosphorylation-based ALPK1 assay to test whether these mutations have an impact on the kinase activity of ALPK1 in resting conditions or after cell treatment with ADPH. For this, c.710C>T and c.3275T>C were introduced into a myc-hALPK1 cDNA construct by directed mutagenesis and corresponding p.T237M and p.V1092A ALPK1 mutants were generated. For each of them, the kinase activity was measured. An increase of thiophosphorylation of GST-TIFA and myc-ALPK1 was observed in response to ADPH sensing, indicating that these mutants exhibit enhanced ADPH-induced kinase activity. These last results are consistent with published studies showing that the T237M mutant has a pro-inflammatory phenotype¹⁶ while V1092A activates NF- κ B²¹. No significant increase in kinase activity was observed in absence of ADPH

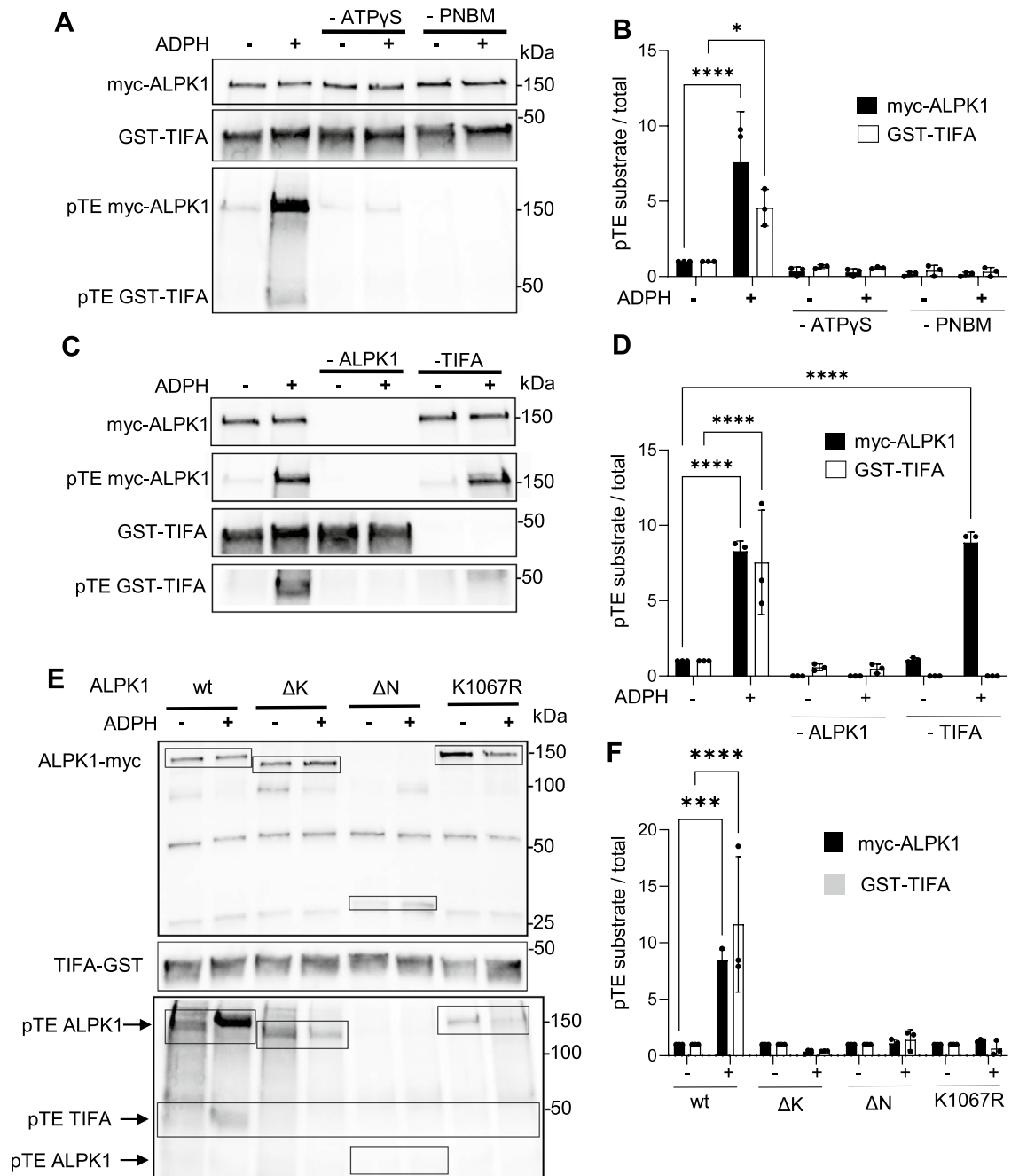


Figure 2. In vitro kinase assay based on protein thiophosphorylation reveals the phosphorylation of ALPK1 in response to ADPH sensing. (A) TIFA and ALPK1 are thiophosphorylated in response to ADPH sensing. HEK293 cells, transfected with a myc-hALPK1 cDNA construct, were treated or not with ADPH for 30 min. myc-ALPK1 was immunoprecipitated and incubated with GST-TIFA \pm ATP γ S and \pm PNBM. Anti-myc, anti-GST and anti-pTE antibodies were used in western blot to detect myc-ALPK1, GST-TIFA and thiophosphorylated proteins, respectively. (B) Quantification of protein thiophosphorylation as shown in (A). For GST-TIFA or myc-ALPK1, protein thiophosphorylation was quantified by measuring the ratio between corresponding pTE signal and total GST-TIFA or myc-hALPK1, respectively. (C) Protein thiophosphorylation signals are dependent on ALPK1 and TIFA. HEK293 cells were transfected or not with a myc-hALPK1 cDNA construct and treated or not with ADPH. myc-ALPK1 was immunoprecipitated and incubated or not with GST-TIFA in the presence of ATP γ S and PNBM. Anti-myc, anti-GST and anti-pTE antibodies were used in western blot to detect myc-ALPK1, GST-TIFA and thiophosphorylated proteins, respectively. (D) Quantification of protein thiophosphorylation as shown in (C). For GST-TIFA or myc-ALPK1, protein thiophosphorylation was quantified by measuring the ratio between corresponding pTE signal and total GST-TIFA or anti-myc, respectively. (E) TIFA and ALPK1 thiophosphorylation is dependent on the kinase and N-terminal domains of ALPK1 and requires intact kinase activity. HEK293 cells were transfected with wt, Δ K, Δ N and K1067R myc-tagged ALPK1 cDNA constructs and were treated or not with ADPH. myc-ALPK1, GST-TIFA and thiophosphorylated proteins were detected as in (A). (F) Quantification of protein thiophosphorylation as shown in (E). GST-TIFA and myc-ALPK1 thiophosphorylation was quantified as in (B). All data correspond to the mean \pm SD of 3 independent experiments. Statistical significance against the untreated wt condition was assessed using two-way ANOVA (B,D,F) followed by Tukey's multiple comparisons test * P < 0.05, *** P < 0.001 **** P < 0.0001.

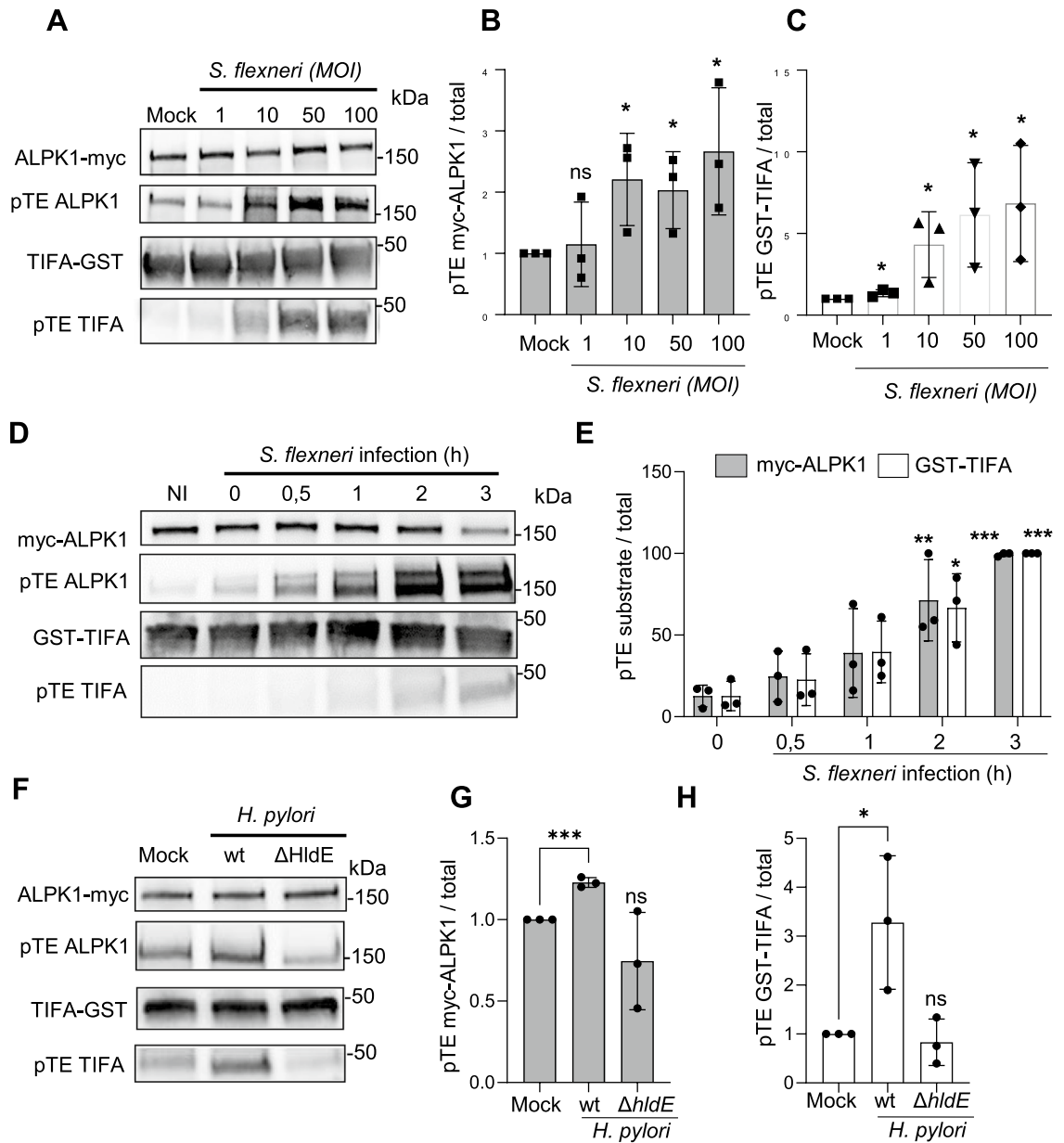


Figure 3. *S. flexneri* and *H. pylori* infections induce the phosphorylation of ALPK1 and TIFA. (A) ALPK1 activity is enhanced in response to increasing *S. flexneri* MOIs. HEK293 cells, transfected with a myc-hALPK1 cDNA construct, were infected or not with wt *S. flexneri* at indicated MOIs for 1 h. ALPK1 kinase activity was then assessed by the newly described protein thiophosphorylation assay. (B) Quantification of myc-ALPK1 thiophosphorylation. (C) Quantification of GST-TIFA thiophosphorylation. (D) ALPK1 activity is sustainably enhanced during *S. flexneri* infection. HEK293 cells, transfected with a myc-hALPK1 cDNA construct, were infected or not with wt *S. flexneri* for indicated time-periods at MOI 10. ALPK1 kinase activity was then assessed by the newly described protein thiophosphorylation assay. (E) Quantification of myc-ALPK1 and GST-TIFA thiophosphorylation. (F) ALPK1 activity is increased during *H. pylori* infection of cells in an ADPH-dependent manner. HEK 293T cells transfected with a myc-hALPK1 cDNA construct, were infected or not with wt or an $\Delta hldE$ *H. pylori* mutant at MOI 20 for 4 h. ALPK1 kinase activity was then assessed by the newly described protein thiophosphorylation assay. (G) Quantification of myc-ALPK1 thiophosphorylation as shown in (F). (H) Quantification of GST-TIFA thiophosphorylation as shown in (F). All data correspond to the mean \pm SD of 3 independent experiments. Statistical significance was assessed between mock and each condition individually using unpaired *t* test (B,C,G,H) or using two-way ANOVA (E) followed by Tukey's multiple comparisons test, * $P < 0.05$, ** $P < 0.01$, *** $P < 0.001$.

treatment (Fig. 5A–C and Supplementary Fig. S12), suggesting that these mutants were not constitutively activated. However, since a bulk biochemistry assay may mask weak responses from some cells expressing

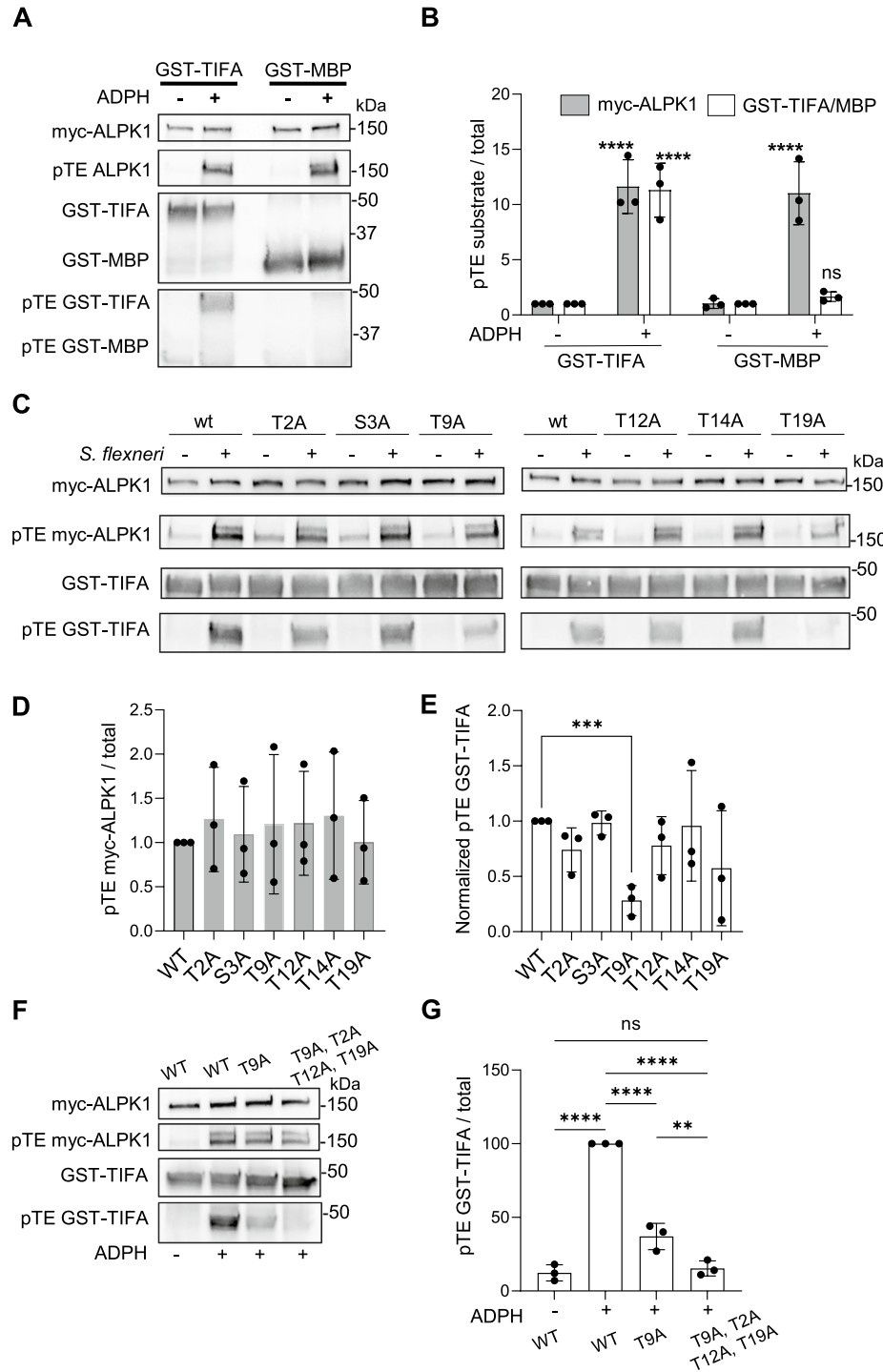


Figure 4. ALPK1 phosphorylates TIFA on multiple residues. (A) MBP is not phosphorylated by ALPK1. HEK cells, transfected with a myc-hALPK1 cDNA construct, were treated or not with ADPH for 30 min. ALPK1 kinase activity was then assessed by incubating immunoprecipitated myc-hALPK1 with TIFA-GST or MBP. (B) Quantification of myc-hALPK1, hTIFA-GST or MBP thiophosphorylation as shown in (A). (C) ALPK1 phosphorylates TIFA on multiple residues. HEK293 cells were transfected with a myc-hALPK1 cDNA construct, myc-hALPK1 was immunoprecipitated and incubated with wt, T2A, S3A, T9A, T12A, T14A or T19A GST-TIFA purified proteins. (D) Quantification of myc-hALPK1 thiophosphorylation as shown in (C). (E). Quantification of GST-TIFA thiophosphorylation as shown in (C). pTE GST-TIFA were normalised to corresponding total GST-TIFA and pTE myc-hALPK1 signals. Data correspond to the mean \pm SD of 3 independent experiments. (F) ALPK1 phosphorylates TIFA on multiple residues. Cells were treated as in (C). Thiophosphorylation assay was performed with wt, T9A and T9A/T12A/T14A/T19A GST-TIFA purified proteins as substrates. (G) Quantification of GST-TIFA thiophosphorylation as shown in (F). Data correspond to the mean \pm SD of 3 independent experiments. Statistical significance was assessed using one-way ANOVA followed by Dunnett’s multiple comparisons test (G), or two-way ANOVA followed by Tukey’s multiple comparisons test (B). Statistical significance was assessed between mock and each condition individually using unpaired *t* test (D,E). **P* < 0.05, ***P* < 0.01, ****P* < 0.001.

ALPK1 mutants, we monitored ALPK1 activity with a single-cell functional assay. For this, the ability of T237M and V1092A ALPK1 mutants to trigger the constitutive formation of TIFAsomes was analysed. HeLa cells stably expressing GFP-hTIFA were depleted of endogenous ALPK1 and transiently transfected with wt, T237M or V1092A myc-hALPK1 cDNA constructs. After fixation, cells were analysed by microscopy and the fraction of cells with TIFAsomes was quantified. Interestingly, some TIFAsomes were observed in a large fraction of cells expressing V1092A (Fig. 5D,E). In addition, a few TIFAsomes were also visible in a small fraction of cells expressing the T237M mutant but this was not statistically significant (Fig. 5D,E). Altogether, we showed that several ALPK1 mutants associated with diseases have an altered ADPH-induced kinase activity and that the V1092A mutant, more particularly associated with spiradenoma and spiradenocarcinoma, induces massive assembly of TIFAsomes in a constitutive manner.

Discussion

ALPK1 is a kinase that is receiving increasing attention in the field of biomedical research. Yet, few studies investigate its activity during infection or in non-infectious diseases. Here, we used a versatile non-radioactive *in vitro* kinase assay that potentially allows to measure ALPK1 kinase activity towards any substrates. Based on thiophosphorylation reactions, it confirmed that pT9 TIFA is a substrate of ALPK1. Interestingly, we found that ALPK1 itself is thiophosphorylated in response to ADPH treatment. Although we can not exclude that ALPK1 may be phosphorylated by another kinase that could be pulled-down with ALPK1 during the immunoprecipitation process, the observation that this mechanism depends on the kinase activity of ALPK1 strongly suggests that ALPK1 is autophosphorylated upon ADPH-induced activation. Consistent with this finding, a study by Snelling et al. published while our manuscript was in preparation also reported that ALPK1 phosphorylates itself upon ADPH recognition²⁸. More work is needed to characterize the precise mechanism of autophosphorylation. In general, autophosphorylation can occur in *cis* when a kinase's own active site catalyzes the phosphorylation reaction, or in *trans* when another kinase of the same kind provides the active site that carries out the enzymatic reaction. Determining whether ALPK1 can form dimers will be critical as trans-autophosphorylation is more frequent when kinase molecules dimerize. More work will also be needed to identify the residues that are autophosphorylated in response to ALPK1 activation. Analysis of ALPK1 activity during *S. flexneri* infection showed that this PRR is activated within minutes of infection and that activation is maintained for several hours, most likely reflecting sustained ADPH release from intracellular bacteria. This may result from residual lysis, active replication of intracellular bacteria or secretion via their T3SS, as previously suggested²⁹. The use of the ALPK1 *in vitro* kinase assay reveals that T9 is not the only residue that is phosphorylated by ALPK1 in response to ADPH sensing. Data showed that T2, T12 and T19 are also weakly phosphorylated by ALPK1. In response to TNF α stimulation, Huang et al. found that T9 is the only phosphorylated residue within the T9-containing peptide (¹MTSFEDADTEE¹¹), indicating that T2 is not phosphorylated⁶. However, it should be noted that ALPK1 is not activated in response to TNF α ⁷ and therefore, this is not the kinase that phosphorylates TIFA in this pathway. Interestingly, imaging experiments performed with alanine substitution mutants of T2, T12 and T19 residues revealed that they are not involved in the formation of TIFAsomes, confirming that T9 is the central residue in this important process observed in response to ADPH sensing. The impact of T2, T12 and T19 phosphorylation remains to be elucidated. Interestingly, Snelling et al. showed that ALPK1 also phosphorylates TIFA at Thr177, a residue located within the TRAF6-binding motif²⁸. Its mutation to aspartic acid prevents TRAF6 but not TRAF2 binding, indicating a role in restricting ADP-heptose signalling. The phosphorylation of Thr177 was not directly tested in our study. However, data showing that the thiophosphorylation of T2A, T12A, T19A and T9A quadruple mutant was not significantly enhanced over the untreated wt TIFA condition suggested that no other amino acids were phosphorylated following ADPH recognition (Fig. 4E,G). Why phosphorylation at Thr177 was not detected by our experimental protocol remains to be explored.

We used the newly developed kinase assay to measure the activity of disease-associated ALPK1 mutants. Interestingly, we found that both T237M and V1092A exhibit an increase of kinase activity with the latter having the strongest effect. In addition to this bulk assay, imaging experiments monitoring the formation of TIFAsomes in single cells in absence of ADPH treatment showed that V1092A, and to a much lesser extent T237M, can induce a constitutive formation of TIFAsomes. T237 is positioned within the ADPH binding site of ALPK1 whereas V1092 is located in the α -kinase domain. Results obtained with these mutants are in line with their phenotypes in the diseases to which they are associated. T237M is responsible for a NF- κ B-mediated autoinflammatory disease in which nearly all patients exhibited at least one feature consistent with inflammation³⁰. V1092A, associated with spiradenomas, is also responsible for constitutive NF- κ B activation²¹. Our data indicate that for both ALPK1 mutants, constitutive activation of NF- κ B is likely due to constitutive formation of TIFAsomes.

In conclusion, this study uses a non-radioactive assay to analyse the kinase activity of ALPK1. It allows us to show that ALPK1 is likely autophosphorylated in response to ADPH recognition and that it can phosphorylate T9 but also additional residues of TIFA. In addition, this assay can be combined with an image-based single cell assay monitoring the formation of TIFAsomes to characterize the basal kinase activity of ALPK1 mutants associated with diseases. Since this assay is not focused to the phosphorylation of one protein in particular, it could be used to identify new substrates of ALPK1 and thereby characterize additional cellular pathways regulated by this kinase involved in health and disease.

Methods

Cell culture and reagents. HEK293 and HeLa cells (American Type Culture Collection) were cultured in Dulbecco's modified Eagle's medium (DMEM) supplemented with 10% fetal calf serum, 2 mM GlutaMAX-1, 100 μ g/mL streptomycin and 100 U/mL penicillin (complete growth medium) at 37 °C under 5% CO₂. HeLa cells

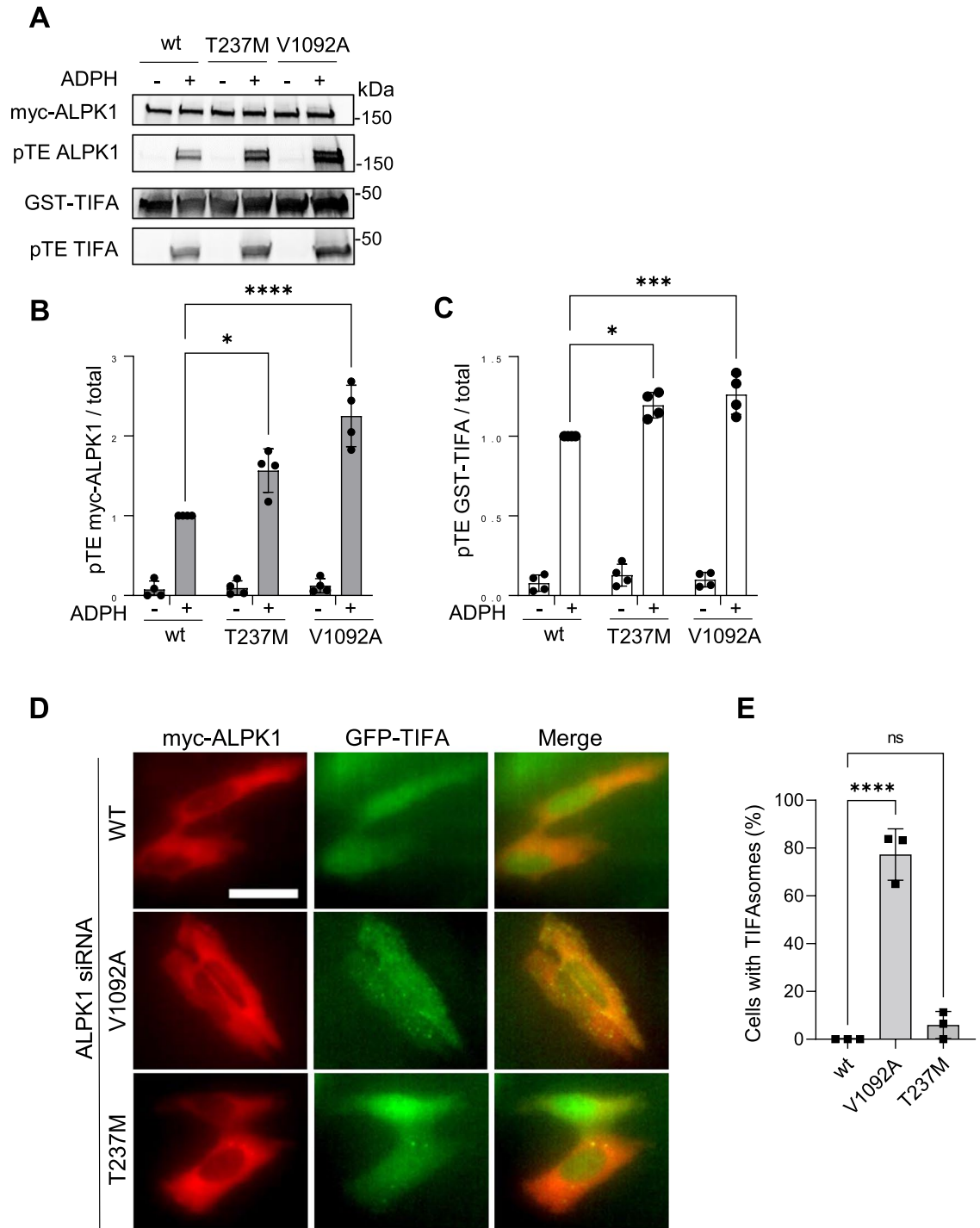


Figure 5. Disease-associated ALPK1 mutants have altered kinase activity. (A) Disease-associated mutants have altered myc-ALPK1 and GST-TIFA thiophosphorylation. HEK293 cells transfected with wt or indicated mutated myc-hALPK1 constructs and treated or not with ADPH. ALPK1 kinase activity was then assessed using the newly described protein thiophosphorylation-based assay. (B) Quantification of myc-hALPK1 thiophosphorylation as shown in (A). (C) Quantification of GST-TIFA thiophosphorylation as shown in (A). (D) V1092A mutant induces constitutive assembly of TIFAsomes. GFP-TIFA-expressing HeLa cells were depleted of endogenous ALPK1 by siRNA and transfected with wt, T237M and V1092A myc-tagged hALPK1 constructs. After 12 h of transfection, cells were fixed without ADPH treatment and stained for myc. TIFA is in green, myc-ALPK1 in red. Bar is 30 μ m. (E) Quantification of cells with TIFAsomes. For each construct, $n > 150$ cells expressing a myc-hALPK1 construct were selected and the fraction of cells with TIFAsomes was quantified. Data correspond to the mean \pm SD of 4 (B,C) or 3 (E) independent experiments. Statistical significance was assessed using two-way ANOVA followed by Tukey's multiple comparisons (B,C) or one-way ANOVA followed by Dunnett's multiple comparisons test (E).

stably expressing GFP-TIFA were previously described⁸. Cells were not cultured in the presence of antibiotics when co-incubated with live *H. pylori*. Pure ADP-heptose was purchased at J&K Scientific BVBA (#9020852) and Invivogen (tlrl-adph-I).

Bacterial strains. DsRed-expressing wild-type (wt) M90T *S. flexneri* and wt and $\Delta hldE$ *H. pylori* strains were described previously^{4,10}.

ALPK1 and TIFA cDNA constructs. Wt or mutated human (h)ALPK1 cDNA constructs were cloned into the pCMV-myc plasmid (Takara Bio Inc) and were all siRNA resistant against the hALPK1 siRNA (s37074) from Ambion (Thermo Fisher Scientific)⁴. In the ΔN ALPK1 mutant (1017–1237), the N-terminal domain of ALPK1 was deleted. It was generated using SalI and NotI restriction enzyme sites which were added by PCR using primers listed in Table 1. The PCR product was then digested with SalI and NotI and ligated into pCMV-myc vector. The ΔK ALPK1 mutant was also generated using SalI and NotI restriction enzymes for cloning. K1067R, T237M and V1092A mutants of ALPK1 were generated by using the QuikChange XL mutagenesis kit (Agilent Technologies, # 200516) and the primers described in Table 1. Wt and T9A GST-TIFA cDNA were generated by cloning into pGEX-4T3 plasmid (kindly provided by F. Margottin, Institut Cochin, France). Wt and T9A pCMV-myc-TIFA cDNA constructs⁴ were used as PCR templates for cloning. Briefly, SalI and NotI restriction enzyme sites were added at each extremity of the genes by PCR using primers described in Table 1. PCR products were then digested with SalI and NotI and ligated into pGEX-4T3 vector. Single mutants T2A, S3A, T9A, T12A, T14A, T19A of TIFA were also generated with the QuikChange XL mutagenesis kit. Quadruple GST-TIFA T9A, T12A, T14A, T19A mutant was obtained by three sequential rounds of directed mutagenesis.

Transfection and rescue experiments. HEK293 cells were seeded at 400,000 cells per well in 6-well plates and transfected the day after with indicated cDNA constructs with FuGENE6 (Roche). Reverse transfection of siRNAs was carried out using RNAiMAX according to the manufacturer's instructions (Invitrogen Thermo Fisher Scientific). Briefly, HeLa cells, seeded in 96-well plates (8000 cells/well), were reverse-transfected with 20 nM siRNA and used 72 h post transfection. As previously described⁴, cells were transfected with a non-targeting siRNA sequence (4390843) or ALPK1 siRNA (s37074) from Ambion (Thermo Fisher Scientific). To replace endogenous ALPK1 by wt or mutated ALPK1, cells were first transfected with ALPK1 siRNA (s37074). Then, 48 h later, they were transfected with siRNA-resistant wt, T237M or V1092A mutated hALPK1 cDNA constructs using FuGENE 6 (Roche).

Purification of GST-TIFA proteins. Thermocompetent *E. coli* BL21 were transformed with wt and mutated pGEX-4T3-GST-TIFA constructs. For each construct, several colonies were cultivated in LB medium containing ampicillin at 100 $\mu\text{g}/\text{mL}$. When bacteria reached an OD_{600} value of 0.4, they were induced with 0.2 M IPTG and incubated at 16 °C over night under agitation. Bacterial cultures were then centrifuged at 6000 $\times g$ for 20 min at 4 °C and pellets were frozen at –20 °C overnight. They were then thawed and resuspended in cold lysis buffer containing PBS 1 \times , 2% Triton X-100, 1 mM PMSF and 2 mg/mL lysozyme (Sigma) and incubated for 1 h on ice. Then, lysates were sonicated (3 pulses of 30 s with 30 s-breaks and 40% amplitude). Sonicated lysates were centrifuged at 16,000 $\times g$ for 30 min at 4 °C. Supernatants were filtered using 0.45 μm syringe filters. Protein purification was performed using glutathione sepharose 4B resin according to the manufacturer's instructions (GE Healthcare). Eluted proteins were then dialyzed and concentrated using an Amicon Ultra-15 10 kDa cutoff (Millipore).

Permeabilized cell assay for ADPH treatment. Cells were treated as previously described⁸. Briefly, cells were washed in permeabilization buffer containing 100 mM KCl, 3 mM MgCl_2 , 50 mM HEPES, 0.1 mM DTT, 85 mM sucrose, 0.2% BSA, and 0.1 mM ATP. They were then incubated with digitonin (2.5 $\mu\text{g mL}^{-1}$) plus ADPH at the desired concentration (J&K Scientific BVBA, #9020852) for 30 min in this same buffer. According to the experiment, cells were then fixed or washed and incubated in DMEM supplemented with 1% FCS for indicated durations.

Bacterial infections. For *S. flexneri* infection, bacteria were used in exponential growth phase and coated with poly-L-lysine prior to infection, as previously described⁴. Cells were seeded in 6-well plates and infected at the indicated multiplicities of infection (MOIs) in DMEM supplemented with 10 mM HEPES, 2 mM GlutaMAX-1 and 1% FCS. After adding bacteria, plates were centrifuged for 3 min at 300 $\times g$ and placed at 37 °C for the indicated times. Cells were then lysed in 1 mL of 1% NP-40 lysis buffer and cell lysates processed for immunoprecipitation and in vitro kinase assay. *H. pylori* infection experiments were carried as previously described¹⁰. Briefly, HEK 293 cells were seeded at 1×10^6 cells per well in 6-well plates and let multiply over night to a confluency of the monolayer of roughly 50–70%. Cells were transfected with myc-hALPK1 construct or empty vector, using lipofectamine 2000 (Invitrogen) according to the manufacturer's instructions. Cells were left to express the ALPK1 construct for 48 h after transfection. Subsequently, freshly grown *H. pylori* (strain N6, wt and *hldE* mutant) was coincubated with the cells, in parallel with mock-infected controls, at an MOI of 20 bacteria per cell. After 4 h of coincubation, cells after medium removal were immediately harvested in 1% NP40-RIPA buffer (800 μL), lysed for 30 min on ice, snap-frozen in liquid nitrogen, and further processed for in vitro kinase assay and protein analysis. Cell protein content of the cleared lysates was determined using BCA assay. Uniform ALPK1 expression was subsequently monitored for all samples using Western immuno-blot on equal

cDNA templates	Constructs	Mutation	Primer sequences or references
pCMV myc-ALPK1	pCMV myc-K1067 ALPK1	K1067	5'-GCTCCTTATAGTCTCTCCCAACATACC TCCCAGA-3' 5'-TCTGGGGAGGTATGTTGGGAGAGA CTATAAGGAGC-3'
pCMV-myc-ALPK1	pCMV-myc-T237M ALPK1	T237M	5'-CCAGTATACCTAGCGACATGGAGA GGCCCTTTTTA-3' 5'-TAAAAAGGGCCTCTCCATGTCGCT AGGTATACTGG-3'
pCMV-myc-ALPK1	pCMV-myc-V1092A ALPK1	V1092A	5'-CTCTTGT TAAAT TCTGTGCGCATAGTGC TGTGCGGC-3' 5'-GACCGCACAGCACTATGCGACAGA ATTAAACAAGAG-3'
pCMV-myc-ALPK1	pCMV-myc-ALPK1 ΔN	ΔN	5'-CCCCTCGACGAAATATCAAAAA ATCTGAACTGTGGACGGCC-3' 5'-GGCGGCCGCTCAAGGTCTAGTCAA AGAAAGCATGGCAGATTTC 3'
pCMV-YFP-ALPK1	pCMV-myc-ALPK1 ΔK	ΔK	5'-GGCGTCGACGATGAATAATCAAAA AGTGGTAGCTGTGC-3' 5'-AAGCGGCCGCTCATAACAAAAGAG CACTATG-3'
pCMV-myc-TIFA	pGEX GST-TIFA		5'-GGGGTCGACATGACCAGT TTTGAA GATGCTGAC-3' 5'-GGCGGCCGCTCATGACTCATTTT CATCCATTTC-3'
pCMV-myc- T9A TIFA	pGEX GST-T9A TIFA		5'-GGGGTCGACATGACCAGT TTTGAA GATGCTGAC-3' 5'-GGCGGCCGCTCATGACTCATTTT CATCCATTTC-3'
pGEX GST-TIFA	pGEX GST-T2A TIFA	T2A	5'-GCATCTTCAAACTGGCCATGTCG ACCCGGGA-3' 5'-TCCCGGGTCGACATGGCCAGTTTT GAAGATGC-3'
pGEX GST-TIFA	pGEX GST-S3A TIFA	S3A	5'-TGT CAGCATCTTCAAAAGCGGTCA TGTGACCCGGG-3' 5'-CCC GGTTCGACATGACCGTTTTG AAGATGCTGACA-3'
pGEX GST-TIFA	pGEX GST-T12A TIFA	T12A	5'-ATGCTGACGCAGAAGAGGCAGTAA CTTGTCTCCAG-3' 5'-CTGGAGACAAGTTACTGCCTCTTC TCCGTCAGCAT-3'
pGEX GST-TIFA	pGEX GST-T14A TIFA	T14A	5'-CGTCATCTGGAGACAAGCTACTGT CTCTTCTGTGT-3' 5'-ACACAGAAGAGACAGTAGCTTGT TCCAGATGACG-3'
pGEX GST-TIFA	pGEX GST-T19A TIFA	T19A	5'-TAACTTGCTCCAGATGGCGGTTT ACCATCTGGC-3' 5'-GCCAGGATGGTAAACCGCCATCTG GAGACAAGTTA-3'
pGEX GST-T9A TIFA	pGEX GST-T9A T2A TIFA	T2A	5'-GCATCTTCAAACTGGCCATGTCG ACCCGGGA-3' 5'-TCCCGGGTCGACATGGCCAGTTTT GAAGATGC-3'
pGEX GST-T9A T2A TIFA	pGEX GST-T9A T2A T12A TIFA	T12A	5'-ATGCTGACGCAGAAGAGGCAGTAA CTTGTCTCCAG-3' 5'-CTGGAGACAAGTTACTGCCTCTTC TCCGTCAGCAT-3'
pGEX GST-T9A T2A T12A TIFA	pGEX GST-T9A T2A T12A T19A TIFA	T19A	5'-TAACTTGCTCCAGATGGCGGTTT ACCATCTGGC-3' 5'-GCCAGGATGGTAAACCGCCATCTG GAGACAAGTTA-3'

Table 1. List of primers used to generate the ALPK1 and TIFA constructs.

amounts of loaded samples with anti-hALPK1 or anti-myc antibodies. The experimental setup was repeated three times (biological replicates) on different days.

In vitro kinase assay with ATP γ S. HEK293 cells were seeded 72 h prior to the experiment at 400,000 cells per well in 6-well plates and transfected the next day with wt or mutated myc-ALPK1 constructs with FuGENE6 (Roche) according to manufacturer's instructions. The day of the experiment, cells were infected or stimulated with ADPH and cells were lysed in a lysis buffer containing 1% NP-40, 150 mM NaCl, 10 mM Tris, 5 mM EDTA, 10% Glycerol, 1 mM vanadate, and Complete Protease Inhibitors (Roche). Total lysates were kept on ice for 20 min and then centrifuged at 16,000g for 30 min. Supernatants were incubated with 1 μ g of mouse monoclonal anti-myc antibody (9E10, Santa Cruz Biotechnology) on a rotating wheel over night at 4 °C to immunoprecipitate myc-tagged ALPK1 proteins. The next day, lysates were incubated with Protein G Dynabeads (Invitrogen Thermo Fisher Scientific) previously equilibrated in lysis buffer on a rotating wheel at 4 °C for 1 h. Immunoprecipitates were washed five times in lysis buffer with the magnet « Dynamag » (Invitrogen) and washed in 1 mL of kinase buffer containing 62.5 mM HEPES, 1.625 mM DTT, 46.9 mM MgCl₂, 3.125 mM EGTA and 15.6 mM beta-glycero-phosphate. For a standard kinase assay reaction, the whole immunoprecipitate was resuspended in 60 μ L of kinase buffer containing 1 μ g of recombinant GST-TIFA and 0.15 mM ATP γ S. This suspension was incubated for 30 min at 37 °C on a rotating wheel. Then, EDTA (20 mM) and the alkylation reagent *para*-nitro-benzyl-mesylate (PNBM, Abcam) at a final concentration of 2.5 mM, were added. The suspension was incubated at room temperature on a rotating wheel for 1 h and then 20 μ L of Laemmli 4 \times containing 20 mM DTT and 2 mM vanadate were added. Samples were kept at -20 °C until immunoblot analysis was performed. GST-MBP was from Sigma.

Immunoblotting. Samples were boiled for 5 min at 95 °C and subjected to SDS-PAGE. Immunoblotting was performed using primary antibodies diluted in phosphate buffered saline containing 0.1% Tween and 5% nonfat dry milk. myc-tagged ALPK1, GST-TIFA and thiophosphorylated proteins were detected with a mouse monoclonal anti-myc antibody (9E10, Santa Cruz Biotechnology), a rabbit polyclonal anti-GST antibody (Abcam, ab19256) and a rabbit polyclonal anti-thiophosphate ester antibody (Abcam, ab92570), respectively. HRP-conjugated secondary antibodies were purchased from GE Healthcare, Cell Signaling technologies or ThermoFisher Scientific. Blots were analysed with an enhanced chemiluminescence method (SuperSignal West Pico Chemiluminescent substrate, Thermo Fisher Scientific). As indicated in the figure legends of the Supplemental information section, some membranes were stripped in stripping buffer (Thermo Fisher Scientific) for 30 min at 37 °C and immunoblotted again as described above.

Immunofluorescence. After fixation in 4% paraformaldehyde, GFP-TIFA-expressing cells were incubated over night at 4 °C in 0.2% saponin with a mouse monoclonal anti-myc antibody (9E10, Santa Cruz Biotechnology) or with a mouse monoclonal NF- κ B p65 antibody (Sc-8008). The day after, cells were washed five times with PBS 1 \times and incubated with secondary antibodies and Hoechst (Life Technologies, H3570) diluted in 0.2% saponin for 45 min. Cells were washed five times in PBS 1 \times and analyzed by microscopy.

Automated microscopy and image analysis. Images were acquired with an ImageXpress Micro (Molecular Devices, Sunnyvale, USA). Quantification of p65 nuclear translocation and cell fraction with TIFAsomes was performed using MetaXpress as previously described^{4,8}. Each data point corresponds to triplicate wells, and more than nine images were taken per well.

Statistical analysis. Data are expressed as mean \pm standard deviation of at least three biological replicates. Tests used to assess statistical significance are described for each figure.

Data availability

The datasets used and/or analysed during the current study are available from the corresponding author on reasonable request.

Received: 5 January 2023; Accepted: 13 April 2023

Published online: 18 April 2023

References

- Middelbeek, J., Clark, K., Venselaar, H., Huynen, M. A. & van Leeuwen, F. N. The alpha-kinase family: An exceptional branch on the protein kinase tree. *Cell. Mol. Life Sci.* **67**, 875–890 (2010).
- Heine, M. *et al.* Alpha-kinase 1, a new component in apical protein transport. *J. Biol. Chem.* **280**, 25637–25643 (2005).
- Lee, C.-P. *et al.* Corrigendum: ALPK1 phosphorylates myosin IIA modulating TNF- α trafficking in gout flares. *Sci. Rep.* **6**, 27323 (2016).
- Milivojevic, M. *et al.* ALPK1 controls TIFA/TRAF6-dependent innate immunity against heptose-1,7-bisphosphate of gram-negative bacteria. *PLoS Pathog.* **13**, e1006224 (2017).
- Takatsuna, H. *et al.* Identification of TIFA as an adapter protein that links tumor necrosis factor receptor-associated factor 6 (TRAF6) to interleukin-1 (IL-1) receptor-associated kinase-1 (IRAK-1) in IL-1 receptor signaling. *J. Biol. Chem.* **278**, 12144–12150 (2003).
- Huang, C.-C.F. *et al.* Intermolecular binding between TIFA-FHA and TIFA-pT mediates tumor necrosis factor alpha stimulation and NF- κ B activation. *Mol. Cell. Biol.* **32**, 2664–2673 (2012).
- Zhou, P. *et al.* Alpha-kinase 1 is a cytosolic innate immune receptor for bacterial ADP-heptose. *Nature* **561**, 122–126 (2018).
- Garcia-Weber, D. *et al.* ADP-heptose is a newly identified pathogen-associated molecular pattern of *Shigella flexneri*. *EMBO Rep.* **19**, e46943 (2018).
- Pfannkuch, L. *et al.* ADP heptose, a novel pathogen-associated molecular pattern identified in *Helicobacter pylori*. *FASEB J. Off. Publ. Fed. Am. Soc. Exp. Biol.* **33**, 9087–9099 (2019).

10. Stein, S. C. *et al.* *Helicobacter pylori* modulates host cell responses by CagT4SS-dependent translocation of an intermediate metabolite of LPS inner core heptose biosynthesis. *PLoS Pathog.* **13**, e1006514 (2017).
11. Gall, A., Gaudet, R. G., Gray-Owen, S. D. & Salama, N. R. TIFA signaling in gastric epithelial cells initiates the cag type 4 secretion system-dependent innate immune response to *Helicobacter pylori* infection. *MBio* **8**, e01168-17 (2017).
12. Zimmermann, S. *et al.* ALPK1- and TIFA-dependent innate immune response triggered by the *Helicobacter pylori* type IV secretion system. *Cell Rep.* **20**, 2384–2395 (2017).
13. Cui, J. *et al.* The ALPK1 pathway drives the inflammatory response to *Campylobacter jejuni* in human intestinal epithelial cells. *PLoS Pathog.* **17**, e1009787 (2021).
14. Ryzhakov, G. *et al.* Alpha kinase 1 controls intestinal inflammation by suppressing the IL-12/Th1 axis. *Nat. Commun.* **9**, 3797 (2018).
15. Sangiorgi, E. *et al.* Rare missense variants in the ALPK1 gene may predispose to periodic fever, aphthous stomatitis, pharyngitis and adenitis (PFAPA) syndrome. *Eur. J. Hum. Genet. EJHG* **27**, 1361–1368 (2019).
16. Williams, L. B. *et al.* ALPK1 missense pathogenic variant in five families leads to ROSAH syndrome, an ocular multisystem autosomal dominant disorder. *Genet. Med. Off. J. Am. Coll. Med. Genet.* **21**, 2103–2115 (2019).
17. Yamada, Y. *et al.* Identification of chromosome 3q28 and ALPK1 as susceptibility loci for chronic kidney disease in Japanese individuals by a genome-wide association study. *J. Med. Genet.* **50**, 410–418 (2013).
18. Fujimaki, T., Horibe, H., Oguri, M., Kato, K. & Yamada, Y. Association of genetic variants of the α -kinase 1 gene with myocardial infarction in community-dwelling individuals. *Biomed. Rep.* **2**, 127–131 (2014).
19. Yamada, Y., Matsui, K., Takeuchi, I., Oguri, M. & Fujimaki, T. Association of genetic variants of the α -kinase 1 gene with type 2 diabetes mellitus in a longitudinal population-based genetic epidemiological study. *Biomed. Rep.* **3**, 347–354 (2015).
20. Liao, H.-F. *et al.* Down-regulated and commonly mutated ALPK1 in lung and colorectal cancers. *Sci. Rep.* **6**, 27350 (2016).
21. Rashid, M. *et al.* ALPK1 hotspot mutation as a driver of human spiradenoma and spiradenocarcinoma. *Nat. Commun.* **10**, 2213 (2019).
22. Ko, A.M.-S. *et al.* ALPK1 genetic regulation and risk in relation to gout. *Int. J. Epidemiol.* **42**, 466–474 (2013).
23. Sondhi, D., Xu, W., Songyang, Z., Eck, M. J. & Cole, P. A. Peptide and protein phosphorylation by protein tyrosine kinase Csk: Insights into specificity and mechanism. *Biochemistry* **37**, 165–172 (1998).
24. Allen, J. J. *et al.* A semisynthetic epitope for kinase substrates. *Nat. Methods* **4**, 511–516 (2007).
25. Sanghera, S., Aebersold, R., Morrison, D., Buresl, E. J. & Pelech, S. L. Identification of the sites in myelin basic protein that are phosphorylated by meiosis-activated protein kinase p44mpk. *FEBS Lett.* **273**, 223–226 (1990).
26. Pietromonaco, S. F., Simons, P. C., Altman, A. & Elias, L. Protein kinase C- θ phosphorylation of moesin in the actin-binding sequence. *J. Biol. Chem.* **273**, 7594–7603 (1998).
27. Kishimoto, A. *et al.* Studies on the phosphorylation of myelin basic protein by protein kinase C and adenosine 3':5'-monophosphate-dependent protein kinase. *J. Biol. Chem.* **260**, 12492–12499 (1985).
28. Snelling, T., Shpiro, N., Gourlay, R., Lamoliatte, F. & Cohen, P. Co-ordinated control of the ADP-heptose/ALPK1 signalling network by the E3 ligases TRAF6, TRAF2/c-IAP1 and LUBAC. *Biochem. J.* **479**, 2195–2216 (2022).
29. Gaudet, R. G. *et al.* Innate recognition of intracellular bacterial growth is driven by the TIFA-dependent cytosolic surveillance pathway. *Cell Rep.* **19**, 1418–1430 (2017).
30. Kozycki, C. T. *et al.* Gain-of-function mutations in ALPK1 cause an NF- κ B-mediated autoinflammatory disease: Functional assessment, clinical phenotyping and disease course of patients with ROSAH syndrome. *Ann. Rheum. Dis.* **81**, 1453–1464 (2022).

Acknowledgements

We gratefully acknowledge financial support from the Agence Nationale pour la Recherche (grants no ANR-14-ACHN-0029-01 and ANR-17-CE15-0006 including postdoctoral fellowships to DGW) and from Fondation ARC pour la Recherche sur le Cancer (grant no ARC—PJA20171206187). We also acknowledge financial support through grant SFB 900 (project no: 158989968), sub-project B6 to CJ by the German Research Foundation. MH was additionally supported by the intramural graduate program “Infection Research on Human Pathogens@MvPI” established at LMU Max von Pettenkofer Institute. We thank Bettina Sedlmaier for expert technical assistance.

Author contributions

D.G.W., C.J. and C.A. designed research. D.G.W., A.S.D., V.T., M.H. and A.C. performed research and analyzed data. D.G.W. and C.A. wrote the manuscript. All authors discussed the results, edited and commented on the article.

Competing interests

The authors declare no competing interests.

Additional information

Supplementary Information The online version contains supplementary material available at <https://doi.org/10.1038/s41598-023-33459-7>.

Correspondence and requests for materials should be addressed to C.A.

Reprints and permissions information is available at www.nature.com/reprints.

Publisher's note Springer Nature remains neutral with regard to jurisdictional claims in published maps and institutional affiliations.



Open Access This article is licensed under a Creative Commons Attribution 4.0 International License, which permits use, sharing, adaptation, distribution and reproduction in any medium or format, as long as you give appropriate credit to the original author(s) and the source, provide a link to the Creative Commons licence, and indicate if changes were made. The images or other third party material in this article are included in the article's Creative Commons licence, unless indicated otherwise in a credit line to the material. If material is not included in the article's Creative Commons licence and your intended use is not permitted by statutory regulation or exceeds the permitted use, you will need to obtain permission directly from the copyright holder. To view a copy of this licence, visit <http://creativecommons.org/licenses/by/4.0/>.

© The Author(s) 2023